RFWD3–Mdm2 ubiquitin ligase complex positively regulates p53 stability in response to DNA damage

Xiaoyong Fu[a,b,1], Nur Yucer[a,b,1], Shangfeng Liu[a,b], Muyang Li[c], Ping Yi[b], Jung-Jung Mu[a,b,3], Tao Yang[a,b], Jessica Chu[a,b], Sung Yun Jung[a,b], Bert W. O'Malley[b], Wei Gu[c], Jun Qin[a,b], and Yi Wang[a,b,2]

[a]Center for Molecular Discovery, Verna and Marrs McLean Department of Biochemistry and Molecular Biology and [b]Department of Molecular and Cellular Biology, Baylor College of Medicine, One Baylor Plaza, Houston, TX 77030; and [c]Institute for Cancer Genetics and Department of Pathology, College of Physicians and Surgeons, Columbia University, 1150 St. Nicholas Avenue, New York, NY 10032

Edited* by Stephen J. Elledge, Harvard Medical School, Boston, MA, and approved January 21, 2010 (received for review October 20, 2009)

In unstressed cells, the tumor suppressor p53 is maintained at low levels by ubiquitin-mediated proteolysis mainly through Mdm2. In response to DNA damage, p53 is stabilized and becomes activated to turn on transcriptional programs that are essential for cell cycle arrest and apoptosis. Activation of p53 leads to accumulation of Mdm2 protein, a direct transcriptional target of p53. It is not understood how p53 is protected from degradation when Mdm2 is upregulated. Here we report that p53 stabilization in the late phase after ionizing radiation correlates with active ubiquitination. We found that an E3 ubiquitin ligase RFWD3 (RNF201/FLJ10520) forms a complex with Mdm2 and p53 to synergistically ubiquitinate p53 and is required to stabilize p53 in the late response to DNA damage. This process is regulated by the DNA damage checkpoint, because RFWD3 is phosphorylated by ATM/ATR kinases and the phosphorylation mutant fails to stimulate p53 ubiquitination. In vitro experiments suggest that RFWD3 is a p53 E3 ubiquitin ligase and that RFWD3–Mdm2 complex restricts the polyubiquitination of p53 by Mdm2. Our study identifies RFWD3 as a positive regulator of p53 stability when the G_1 cell cycle checkpoint is activated and provides an explanation for how p53 is protected from degradation in the presence of high levels of Mdm2.

degradation | E3 ubiquitin ligase | G_1 cell cycle checkpoint | ATM/ATR kinase | RING finger domain

The p53 tumor suppressor is a key regulator of cell cycle arrest and apoptosis in response to genotoxic stress (1–3). The G_1 cell cycle checkpoint is operated through the p53-dependent transcriptional response (4). Accumulation of the p53 target gene product $p21^{WAF1/CIP1}$ after DNA damage to a suprathreshold level, capable of blocking the G_1-S promoting cyclinE/Cdk2 activity, may require several hours and is responsible for the sustained G_1 arrest (5).

p53 is primarily regulated at the level of protein stability (6, 7). At least five E3 ligases (E6-AP, Mdm2, Arf-BP1, COP1, and Pirh2) have been identified to mediate ubiquitin-dependent proteasomal degradation of p53. Each of the E3 ligases is capable of building K48-linked polyubiquitin chains on p53, which are recognized by 26S proteasome for degradation. In response to DNA damage, it is thought that such polyubiquitination is inhibited to stabilize p53 protein. Mdm2 is the major p53 E3 ligase, because embryonic lethality of Mdm2-knockout mice caused by p53-induced apoptosis is rescued by deletion of p53 (8, 9).

One paradox exists in the Mdm2 axis for p53 stabilization. Because Mdm2 is a p53 transcription target, stabilization of p53 leads to up-regulation of Mdm2 (10), which in turn should degrade p53, but p53 is maintained at high levels when the G_1 checkpoint is active. It was proposed that DNA damage destabilizes Mdm2 by a mechanism involving phosphorylation by ATM/ATR and increased Mdm2 turnover. Thus, accelerated Mdm2 ubiquitination shortens its half-life, suppressing its activity towards p53 (11). Posttranslational modification of p53 is another important mechanism for its regulation (6). p53 modification by phosphorylation, acetylation, methylation, sumoylation, and neddylation may disrupt p53–Mdm2 interaction or inhibit p53 ubiquitination if the same lysine residues are modified by acetylation (12). It is noteworthy that all known E3 ligases are negative regulators of p53 by promoting p53 degradation, which is inhibited in response to DNA damage. Here we show that E3 ligase RING finger and WD repeat domain 3 (RFWD3), a substrate of checkpoint kinase ATM/ATR and a regulator of the G_1-S checkpoint (13, 14) protects p53 from degradation in the presence of high levels of Mdm2.

Results

RFWD3 Is Phosphorylated by ATM/ATR in Response to DNA Damage. To demonstrate that RFWD3 is a substrate of the checkpoint kinase ATM/ATR, we inhibited ATM activity by pretreating the cells with an ATM-specific inhibitor KU55933. RFWD3 phosphorylation was inhibited at 1 h after IR but was not affected at later times (Fig. 1*A*). Consistent with these data, RFWD3 phosphorylation was largely maintained in an ATM stable knockdown cell line (Fig. 1*A*). Next, we knocked down ATR by siRNA in HeLa cells and found that RFWD3 was phosphorylated in the absence of IR (Fig. 1*B*), possibly because of the induced stress by the loss of ATR that activates other PI-3-like kinases, including ATM. Importantly, IR-induced RFWD3 phosphorylation was abolished as a result of ATR knockdown; when both ATM and ATR were depleted, both basal level and IR-induced RFWD3 phosphorylation were eliminated (Fig. 1*B*). An in vitro kinase assay showed that GST-RFWD3 purified from *Escherichia coli* was phosphorylated by wild-type ATR but not by ATR-KD (kinase dead) mutant (Fig. 1*C*).

RFWD3 contains a RING finger domain and displays in vitro E3 ubiquitin ligase activity (Fig. S1*A* and *B*). In addition, it has an SQ-rich region in the N terminus, a coiled-coil domain, and a WD40 domain in the C terminus. Sequence comparison revealed that the residues flanking serine 46 and serine 63 (S46 and S63) of RFWD3 resemble those around BRCA1 serine 1457 (Fig. S2*A*), suggesting that they might be the phosphorylation sites recognized by the anti-BRCA1-phospho-S1457 antibody. Note that the size of the trypsin-digested peptide containing S46 and S63 (residue 1–97) is approximately 10 kDa, which is too large to be detected by the ion-trap mass spectrometry. To map the phosphorylation sites, we mutated both S46 and S63 to alanines (RFWD3-2SA)

Author contributions: X.F., N.Y., J.Q., and Y.W. designed research; X.F., N.Y., S.L., M.L., P.Y., J.-J.M., T.Y., J.C., S.Y.J., J.Q., and Y.W. performed research; B.W.O. and W.G. contributed new reagents/analytic tools; X.F., N.Y., S.L., J.Q., and Y.W. analyzed data; and X.F., J.Q., and Y.W. wrote the paper.

The authors declare no conflict of interest.

*This Direct Submission article had a prearranged editor.

[1]X.F. and N.Y. contributed equally to this work.

[2]To whom correspondence should be addressed. E-mail: yiw@bcm.edu.

[3]Present address: Research and Diagnostic Center, Centers for Disease Control, Department of Health, 161 Kunyang Street, Taipei, Taiwan.

This article contains supporting information online at www.pnas.org/cgi/content/full/0912094107/DCSupplemental.

BIOCHEMISTRY

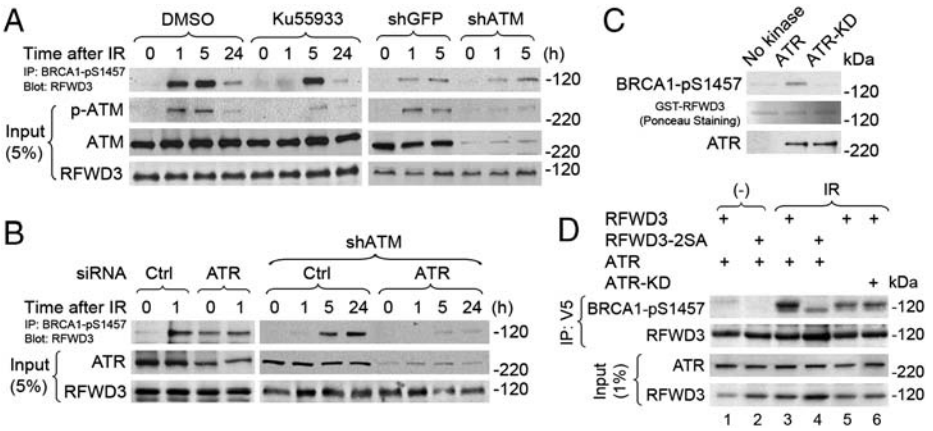

Fig. 1. RFWD3 is phosphorylated by ATM/ATR kinase in response to DNA damage. (*A*) HeLa cells treated by KU55933 1 h before IR or stably knocked down by shATM were irradiated with 10 Gy IR. Phosphorylated RFWD3 was immunoprecipitated by anti-BRCA1-phospho-S1457 antibody and detected by Western blotting with an RFWD3 antibody. (*B*) Transient knockdown of ATR was performed in parental HeLa cells or stable ATM knocked-down HeLa cells. Phosphorylated RFWD3 in response to IR was detected as in *A*. (*C*) In vitro kinase assay was performed with purified Flag-ATR or Flag-ATR-KD protein from transfected 293 T cells and recombinant GST-RFWD3 purified from *E. coli*. (*D*) V5-RFWD3-wild-type or -2SA (S46A/S63A) was cotransfected with ATR or ATR-KD into 293 T cells. RFWD3 was immunoprecipitated with V5 antibody from untreated or 10 Gy IR-treated cells, and its phosphorylation was detected by anti-BRCA1-phospho-S1457 antibody.

and transfected the V5-RFWD3 together with ATR in 293 Tcells. As predicted, RFWD3 phosphorylation following IR treatment was markedly decreased in the RFWD3-2SA mutant (Fig. 1*D*). The residual signal from RFWD3-2SA likely resulted from the phosphorylation at other SQ sites. Consistently, overexpression of ATR enhanced RFWD3 phosphorylation, whereas ATR-KD did not (Fig. 1*D*, compare lanes 3 and 6 to 5), indicating that ATR is responsible for the phosphorylation at these sites under our conditions. Together, our data suggest that whereas ATM phosphorylates RFWD3 at early times upon DNA damage, ATR is the major kinase that phosphorylates RFWD3 at later times.

RFWD3 Interacts with Mdm2 and p53. To dissect the signalling pathway that RFWD3 functions, we isolated the endogenous nuclear RFWD3 complexes from cycling and hydroxyurea (HU)-treated HeLa cells and identified the associated proteins by mass spectrometry (Fig. S2*B*). Two peptides derived from the oncoprotein Mdm2 were found in the HU-treated sample. Next, we confirmed the RFWD3–Mdm2 association by transient cotransfection in 293 T cells. As shown in Fig. S2*C*, immunoprecipitation of V5-RFWD3 brought down Flag-Mdm2. Conversely, V5-RFWD3 could be reciprocally coimmunoprecipitated by anti-Flag IP of Mdm2. Although Mdm2 was originally identified from the endogenous RFWD3 complex in HeLa cells only after HU treatment, overexpressed Mdm2 and RFWD3 could interact either before or after IR treatment, suggesting that the interaction detected by mass spectrometry may be a result of increased Mdm2 protein level in response to genotoxic stress.

Because p53 protein level is kept low by E6-AP-mediated degradation in HeLa cells, we further investigated the endogenous interaction of RFWD3 and Mdm2 in a p53 positive cell line MCF7. Two antibodies (Ab1 and Ab2) against different regions of RFWD3 were able to coimmunoprecipitate Mdm2 from MCF7 nuclear extracts (Fig. 2*A*). Interestingly, p53 was also detected in the RFWD3 immunocomplexes, indicating the formation of an RFWD3–Mdm2–p53 ternary complex. Indeed, reciprocal IP with a p53 antibody brought down both RFWD3 and Mdm2 from cycling MCF7 cells and cells treated by camptothecin (CPT) that causes double-strand DNA breaks (Fig. 2*B*). Furthermore, recombinant GST-RFWD3 was able to pull down Flag-p53 (Fig. 2*C*, lane 3) or His-Mdm2 (lane 4), indicating that RFWD3 can form a binary complex with either p53 or Mdm2; when all three proteins were present, RFWD3 brought down Mdm2 more efficiently than in the absence of p53 (compare lanes 4 and 5, Fig. 2*C*), suggesting that p53 may also contribute to binding between RFWD3 and Mdm2. Domain mapping experiments using deletion mutants suggest that Mdm2 acidic domain is required for its binding to RFWD3 (Fig. 2*D*). Together these data strongly suggest that RFWD3 interacts with Mdm2 and p53 in vivo and in vitro.

RFWD3 Is a Positive Regulator of p53 Abundance and Regulates G_1 Checkpoint in Response to IR. Because ubiquitination of p53 by Mdm2 leads to p53 degradation, we investigated whether RFWD3 also regulates p53 abundance. In both U2OS and MCF7 cells, p53 levels were accumulated after IR albeit with different kinetics. Consistently, the IR-induced p53 accumulation and up-regulation of $p21^{WAF1/CIP1}$ were attenuated by knockdown of RFWD3 with two different siRNAs (Fig. 3*A* and *B*). To further assess the role of RFWD3 in p53-dependent cell cycle arrest, we measured the G_1 checkpoint in RFWD3 knockdown cell lines. The G_1 checkpoint was measured as the ratio of S-phase entry in 4-h time frames after IR to that of cycling cells (Fig. S3*A*). As expected, p53 was required for the G_1 checkpoint, because siRNA-mediated p53 knockdown almost completely abolished the arrest starting from 4 h after IR (Fig. S3*B* and *C*). In contrast, knockdown of RFWD3 had minimal effect on G_1 arrest during the first 8 h after IR but resulted in a 2–3-fold increase in S-phase entry 8–12 h after IR (Fig. 3*C*), suggesting that RFWD3 is required for the G_1 checkpoint maintenance. Importantly, the defective G_1 checkpoint could be rescued by expression of an RNAi-resistant RFWD3 DNA plasmid in a stable RFWD3 knockdown cell line (Fig. 3*D*). These data demonstrate that RFWD3 positively regulates p53 abundance and is required for maintaining G_1 cell cycle arrest in response to IR.

RFWD3 Is also Required to Stabilize Mdm2. Next, we tested whether RFWD3 stabilizes p53 by inactivating Mdm2 in response to DNA damage. We knocked down RFWD3 in U2OS cells and monitored the Mdm2 protein levels after IR. Whereas the Mdm2 accumulation was apparent from 4 h after IR in control knockdown cells, it was compromised in RFWD3 knockdown cells (Fig. 4*A*). Importantly, the defect in Mdm2 accumulation could be rescued by cotransfection of an RNAi-resistant RFWD3 (Fig. 4*B*). Consistently, cotransfection of Mdm2 with RFWD3 in p53-null H1299 cells resulted in more stabilized Mdm2 compared to the transfection of Mdm2 alone, whereas cotransfected RFWD3-CA (C315A mutant in RING domain that abolishes its E3 ligase activity; see below) had much less effect (Fig. 4*C*).

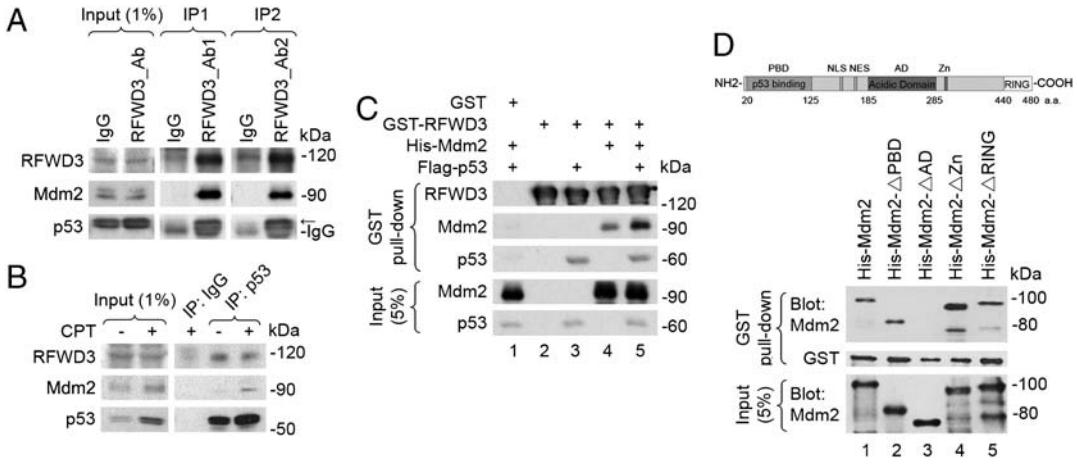

Fig. 2. RFWD3 interacts with Mdm2. (*A*) and (*B*) Coimmunoprecipitation of RFWD3, Mdm2, and p53 was performed with nuclear extracts prepared from untreated or 100 nM CPT-treated MCF7 cells. (*C*) and (*D*) Recombinant Flag-p53, His-Mdm2 (full-length or domain-deletion mutants) were mixed with GST-RFWD3 on beads. Pulled-down proteins were blotted by the indicated antibodies.

We next measured the half-life of Mdm2 as a function of RFWD3 protein levels. In the RFWD3 stable knockdown cells, the Mdm2 half-life was shortened by nearly 2-fold compared to the control cell line (Fig. 4*D*). Conversely, coexpression of RFWD3, not RFWD3-CA, with Mdm2 in H1299 cells extended the half-life of Mdm2 (Fig. 4*E*). Together these data show that RFWD3 is able to stabilize Mdm2 in a RING domain-dependent manner.

RFWD3 Synergizes with Mdm2 to Enhance p53 Ubiquitination in Response to IR. Because RFWD3 is a p53 E3 ligase in vitro (Fig. S1*B*), we investigated whether RFWD3 regulates p53 ubiquitination. We first examined the kinetics of endogenous p53 ubiquitination in response to IR. The ubiquitinated p53 (Ub-p53) generated by multiple E3 ligases exhibits a "ladder" pattern in Western blotting. These bands migrate above 53 kDa and are separated by ~10 kDa as a characteristic of ubiquitination. As shown in Fig. S4*A*, p53 protein started to accumulate as early as 1.5 h after IR and remained at high levels afterwards in U2OS cells. However, the intensity of the Ub-p53 ladder does not strictly correlate with the unmodified p53 after IR. Compared with cycling cells, the intensity of the Ub-p53 ladder decreased sharply 1.5 h after IR, concomitant with initial p53 accumulation. Then the intensity of Ub-p53 ladder started to increase 2.5 h after IR and was maintained at higher levels at later times. Similar patterns of the Ub-p53 ladder were also observed in MCF7 and HCT116 cells, albeit with different kinetics (Fig. S4*B* and *C*). Therefore, p53 stabilization in response to IR appears to be regulated under different mechanisms—stabilization is initiated through complete inhibition of p53 ubiquitination in the early phase but is maintained in the presence of ubiquitination in the late phase. Decreased p53 ubiquitination in the early phase is consistent with the fact that Mdm2 is inactivated after DNA damage through rapid turnover (11). Notably, whereas the

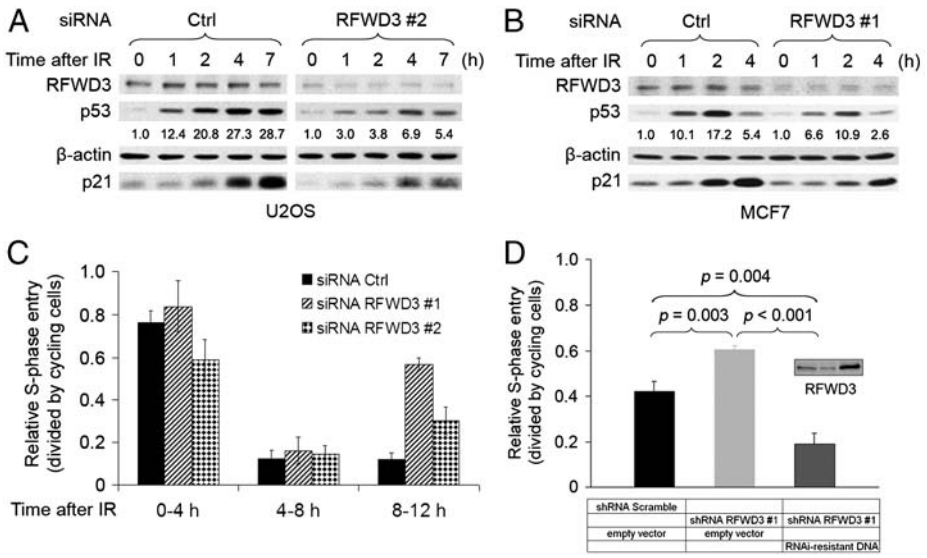

Fig. 3. RFWD3 is a positive regulator of p53 abundance and regulates the G_1 checkpoint in response to IR. (*A*) U2OS cells were transfected with a RFWD3 siRNA (sequence no. 2) or control siRNA. At 48 h posttransfection, cells were irradiated with 10 Gy IR. Cell lysates were immunoblotted with indicated antibodies. Quantification of relative p53 levels was normalized by β-actin signals. (*B*) The same experiment as in *A* was performed in MCF7 cells by using a different RFWD3 siRNA (sequence no. 1). (*C*) MCF7 cells were transfected with RFWD3 siRNAs (no. 1 or 2) or a control siRNA. At 48 h posttransfection, cells were irradiated with 2.5 Gy IR. The G_1 checkpoint was measured by the relative S-phase entry at indicated time frames. (*D*) Rescue of the G_1 checkpoint by expressing an RNAi-resistant RFWD3 in U2OS stable shRNA knockdown cells. The cells were transfected with the indicated plasmids and were irradiated with 2.5 Gy IR at 48 hr posttransfection.

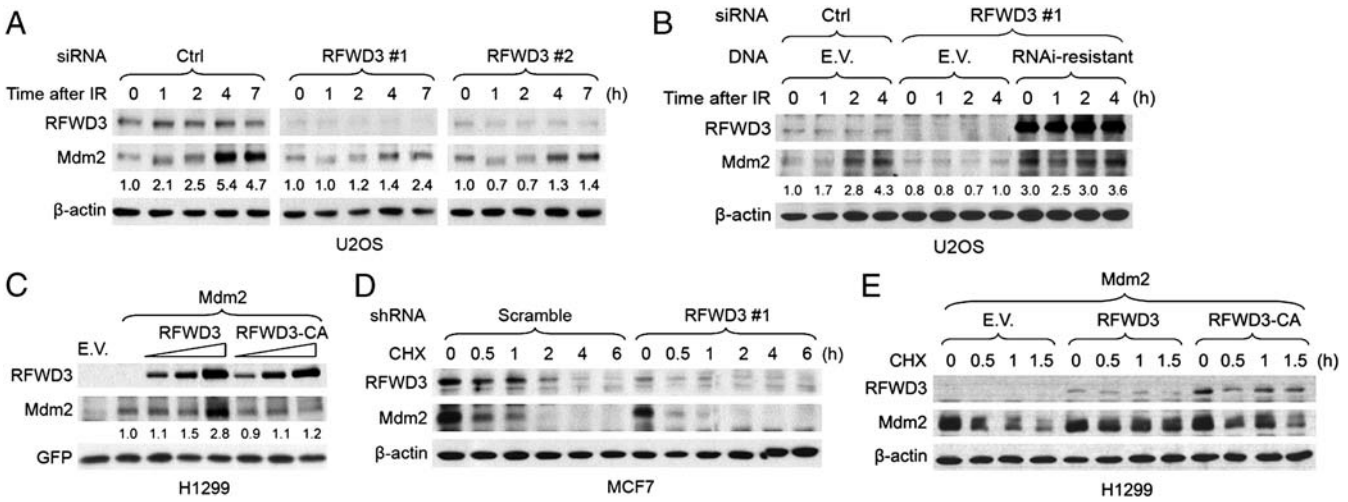

Fig. 4. RFWD3 stabilizes Mdm2. (*A*) U2OS cells were transfected with RFWD3 siRNAs (no. 1 or 2) or control siRNA. At 48 h posttransfection, cells were irradiated with 10 Gy IR. Quantification of relative Mdm2 levels was normalized by β-actin signals. (*B*) U2OS cells were transfected with control siRNA, RFWD3 siRNA (sequence no. 1), together with empty vector (E.V.) or RNAi-resistant RFWD3. At 48 h posttransfection, cells were irradiated with 10 Gy IR and cell lysates were collected at indicated time points. (*C*) H1299 cells were transfected with E.V. or cotransfected with Mdm2 and various amounts of V5-RFWD3 or V5-RFWD3-CA. GFP was used as an internal control for transfection efficiency. The relative Mdm2 levels were quantified by normalizing to GFP signals. (*D*) MCF7 cells stably transfected with an RFWD3 shRNA (sequence no. 1) or control (scramble) shRNA were treated with cycloheximide for indicated times. (*E*) H1299 cells were transfected with Mdm2 alone or Mdm2 combined with V5-RFWD3 or V5-RFWD3-CA and treated with cycloheximide for indicated times.

Mdm2 half-life was shortened during the early response to IR (2 h after IR), it was considerably prolonged in the late phase (6 h after IR) (Fig. S5), suggesting a positive correlation between Mdm2 half-life and the intensity of Ub-p53 ladder.

To examine the role of RFWD3 and Mdm2 for p53 ubiquitination in the late phase of the response, we knocked down Mdm2, RFWD3, or both and measured the Ub-p53 ladder by Western blotting. Knockdown of either Mdm2 or RFWD3 resulted in decreased intensity of the Ub-p53 ladder in U2OS cells 4 h after IR (Fig. 5*A*; compare lanes 4 and 9 to 2 and 8), and double knockdown of both RFWD3 and Mdm2 led to greater decrease of the Ub-p53 ladder (Fig. 5*A*; compare lane 10 to 8). These data suggest that both RFWD3 and Mdm2 participate in maintaining p53 ubiquitination in the late phase response.

To corroborate the knockdown results, we examined how RFWD3, Mdm2, and their E3 ligase activities affect p53 ubiquitination after IR in overexpression experiments. As shown in Fig. 5*B*, whereas Mdm2 alone readily ubiquitinated p53, RFWD3 alone exhibited nearly undetectable E3 ligase activity towards p53 (Fig. 5*B*, lane 3); coexpression of Mdm2 with RFWD3 resulted in a significant enhancement of p53 ubiquitination (Fig. 5*B*, lane 5), suggesting functional synergy between the two E3 ligases. RFWD3-CA showed minimal stimulation of Mdm2-mediated p53 ubiquitination (Fig. 5*B*, lane 6), and neither Mdm2-CA (a C464A mutant with defective E3 ligase activity) alone nor in

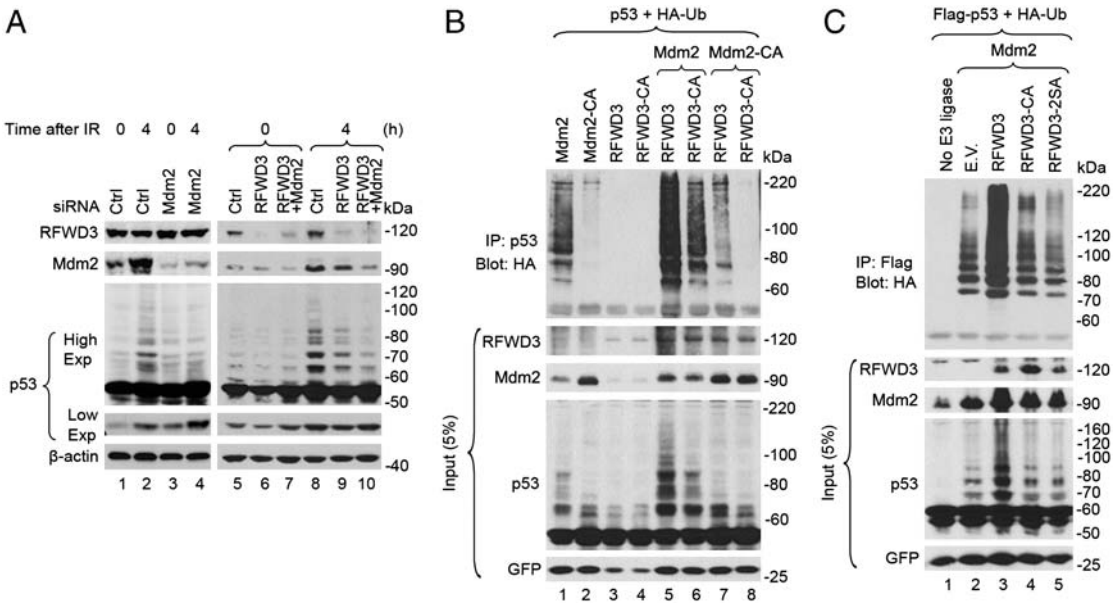

Fig. 5. RFWD3 synergizes with Mdm2 to enhance p53 ubiquitination in response to IR. (*A*) U2OS cells were transfected with indicated siRNA and were irradiated with 10 Gy IR at 48 h posttransfection. A higher exposure (High Exp) of p53 was taken to show the ubiquitination ladders. (*B*) H1299 cells were cotransfected as indicated and irradiated with 10 Gy IR 4 h before cell lysis. Cell lysates were prepared as described in *Experimental Procedures*. Ubiquitinated p53 proteins were immunoprecipitated by anti-p53 antibody and blotted with anti-HA antibody. (*C*) H1299 cells were cotransfected with indicated DNA vectors and irradiated with 10 Gy IR. Flag-p53 was immunoprecipitated with Flag M2 antibody and the ubiquitinated p53 was detected by HA Western blotting.

combination with RFWD3-CA ubiquitinated p53 (lanes 2 and 8), confirming that the E3 ligase activities of both RFWD3 and Mdm2 are required for the observed synergistic effect. Interestingly, coexpression of RFWD3 with Mdm2-CA also led to a low level of p53 ubiquitination (lane 7), raising the possibility that Mdm2-CA acts as an adaptor to present p53 to the overexpressed RFWD3 for ubiquitination. Indeed, GST-RFWD3 purified from *E. coli* exhibited robust E3 ligase activity to p53 without Mdm2 in vitro (Fig. S1*B* and see below).

Finally, we investigated the role of RFWD3 phosphorylation in p53 ubiquitination in response to DNA damage. Compared to wild-type RFWD3, which stimulates p53 ubiquitination, RFWD3-2SA mutant failed to enhance Mdm2-mediated p53 ubiquitination, suggesting that RFWD3 phosphorylation further enhances p53 ubiquitination after IR (Fig. 5*C*, lanes 2, 3, and 5).

RFWD3 Restricts Mdm2 from Extending Polyubiquitin Chain on the Ubiquitinated p53. To further investigate the underlying mechanism of RFWD3-mediated p53 stabilization, we carried out in vitro ubiquitination assay by using recombinant E1, E2 (UbcH5), Flag-p53, GST-RFWD3, and GST-Mdm2 purified from *E. coli*. Consistent with its known function, Mdm2 generated polyubiquitinated p53 species that migrated above 220 kDa in a dosage-dependent manner (Fig. 6*A*, lanes 2–5). In contrast, RFWD3, not its CA mutant, catalyzed the formation of Ub-p53 that migrated at ~100 to 160 kDa (Fig. 6*A*, lanes 7–10). Simultaneous addition of both E3 ligases resulted in a p53 ubiquitination pattern resembling the one generated by Mdm2 alone (Fig. 6*B*; compare lane 6 to 3). In agreement with in vivo results, the efficiency of ubiquitination reaction was enhanced in the presence of both ligases, resulting in further reduction of unubiquitinated p53 (Fig. 6*B*, lane 6).

To test the effect of the RFWD3–Mdm2 complex on p53 ubiquitination, we preincubated RFWD3 with Mdm2 to allow the formation of the complex before the addition of p53 as the substrate. Formation of the RFWD3-Mdm2 complex suppressed the polyubiquitinated p53 that migrated above 220 kDa but enhanced Ub-p53 that migrated between 100 and 220 kDa, consistent with Ub-p53 with shorter ubiquitin chains (Fig. 6*B*, lane 9). In contrast, preincubation of Mdm2 with RFWD3-CA did not cause noticeable changes (Fig. 6*B*, lane 10).

Discussion

The RFWD3–Mdm2 Complex Is a Positive Regulator of p53 Stability in Response to IR. It is generally accepted that the mechanism for p53 stabilization in response to DNA damage is by inhibiting the activity of p53 E3 ubiquitin ligases. We provide evidence here that p53 ubiquitination and stabilization appears to consist of two phases that may be governed by different molecular mechanisms: At early times after IR, p53 ubiquitination is suppressed, which correlates well with the timing of immediate p53 stabilization and Mdm2 inactivation; however, when the p53-dependent transcriptional program is activated and the G_1 checkpoint is engaged, ubiquitination of p53 is restored and correlates with stabilized p53. Published work suggest that the early response is likely regulated through posttranslational modifications of p53 and Mdm2, which result in the dissociation of p53 from Mdm2 and the shortened half-life of Mdm2 (11, 15). The mechanism for the late phase of the response is the topic of this study. We show that RFWD3 E3 ligase stabilizes p53 in response to DNA damage, suggesting that ubiquitination can also positively regulate p53. What is the mechanism underlying RFWD3–Mdm2 complex-catalyzed ubiquitination that stabilizes p53? Our in vitro experiments suggest an interesting scenario. In vitro binding experiments showed that the acidic domain of Mdm2 is required for its binding to RFWD3. Work from several groups demonstrated that Mdm2 acidic domain is also a second binding site for p53 (16–18) and that binding of the acidic domain signals for ubiquitination (17). It is tempting to speculate that RFWD3 binding blocks the interaction between the Mdm2 acidic domain and p53, thus turning off the Mdm2 ubiquitination signal. As an E3 ligase, RFWD3 can catalyze the formation p53-Ub with shorter Ub chains. Because 4 Ub is the minimum targeting length by 26S proteasome, p53-Ub generated by the RFWD3–Mdm2 complex may effectively avoid being recognized and degraded.

The RFWD3–Mdm2 Complex Regulated by DNA Damage Checkpoint Contributes to Maintenance of the G_1 Checkpoint. DNA damage-induced ATM/ATR activation leads to phosphorylation of p53 and Mdm2 at Ser 15 and Ser 395 sites, respectively, which contributes to p53 stabilization and G_1 checkpoint activation (19, 20). As a substrate of the ATM/ATR kinase, RFWD3 function is also likely regulated by the DNA damage checkpoint. Unlike Mdm2, whose phosphorylation by ATM stimulates its rapid autodegradation and abrogates its ubiquitination of p53, the level of

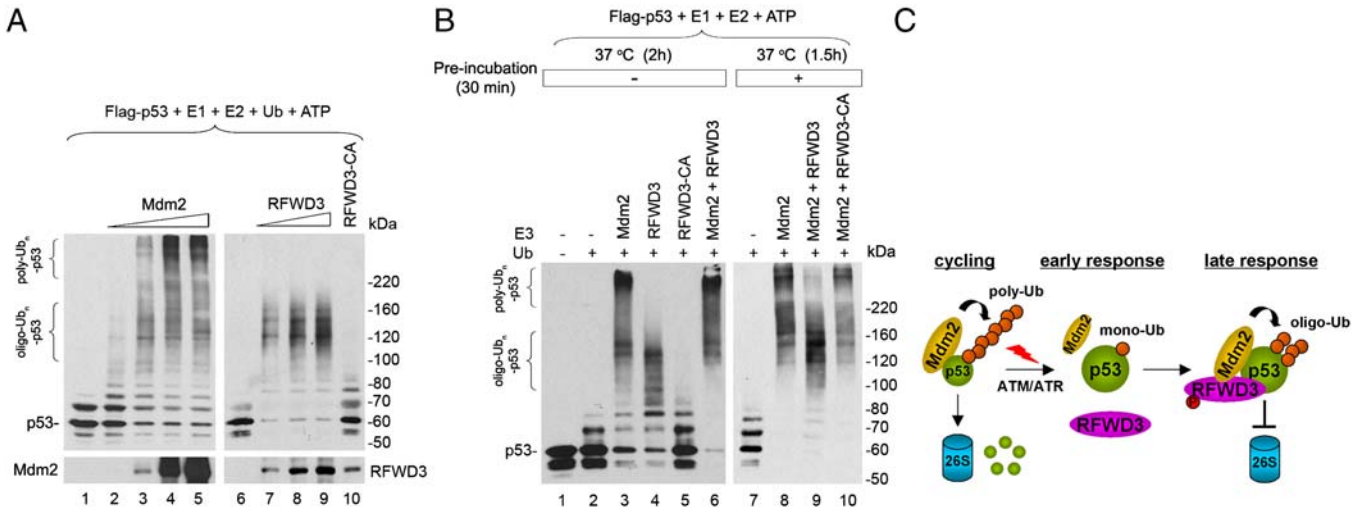

Fig. 6. RFWD3 restricts Mdm2's ability to extend polyubiquitin chain on p53. (*A*) In vitro ubiquitination assay was performed by using Flag-p53 purified from *E. coli* as a substrate and increasing amounts of GST-RFWD3 or GST-Mdm2 as E3 ligases. (*B*) Flag-p53 was incubated with the indicated E3 ligases at 37 °C for 2 h (lanes 1–6); alternatively, all the components except for Flag-p53 were preincubated for 30 min and incubated for another 1.5 h after the addition of Flag-p53 (lanes 7–10). (*C*) Schematic representation of the proposed two-step model for stabilization of p53 in response to IR.

RFWD3 after IR remains largely unchanged. However, the RFWD3-2SA mutant is unable to enhance p53 ubiquitination by Mdm2 after IR, suggesting that phosphorylation of RFWD3 can further regulate p53 stabilization. It is possible that phosphorylation of RFWD3 by ATR may modulate its activity or localization. In this context, RFWD3 may act as a rheostat to maintain the appropriate level of p53. Once the checkpoint is turned off, RFWD3 becomes inactive, allowing Mdm2 to perform its default function to maintain low levels of p53. On the basis of our data and published work, we propose a working model for p53 stabilization in response to IR (Fig. 6*C*). In the early phase of the IR response, posttranslational modification of p53 and Mdm2, as well as accelerated degradation of Mdm2, transiently blocks p53 ubiquitination and thus stabilizes p53. During the late phase of the response, higher concentration of Mdm2, a result of the p53 feedback program, as well as RFWD3 phosphorylation by ATR allows the formation of the RFWD3–Mdm2–p53 ternary complex. This complex modulates Mdm2's E3 ligase activity to restrict the length of ubiquitin chains on p53, thus protecting it from 26S proteasome degradation.

Experimental Procedures

Cell Culture and Chemicals. HEK293 T, HeLa, MCF7, and HCT116 cells were maintained in DMEM, H1299 cells in RPMI medium 1640, and U2OS cells in McCoy's 5A medium. All media were supplemented with 10% fetal bovine serum. The stable cell lines (shRNA knockdown) were maintained in DMEM medium supplemented with 0.5 μg/mL puromycin (Sigma). Cycloheximide (100 μg/mL) and KU55933 (10 μM) were bought from Sigma.

Expression Vectors and Antibodies. Full-length human RFWD3 protein was cloned into pcDNA3.1-V5 (Invitrogen) from a cDNA pool of HeLa cells. p53 and Mdm2 constructs have been described previously (21). Antibodies used in this study were as follows: anti-RFWD3 (BL2378, Bethyl Laboratories; Ab1 and Ab2, CapitalBio Corp.), anti-p53 (DO1 and FL-393; Santa Cruz), anti-p21 (C19; Santa Cruz), anti-β-actin (Sigma), anti-GFP (FL; Santa Cruz), anti-Flag (M2; Sigma), anti-V5 (Bethyl), and anti-HA (Y11; Santa Cruz).

Immunoprecipitation and Mass Spectrometry. HeLa nuclear extracts were prepared as described previously (22). Immunoprecipitations were carried out in 1 mL of nuclear extract with 8 μg antibody. The immunoprecipitates were sequenced with a linear ion-trap (LTQ) mass spectrometry as described (23).

RNA Interference. siRNA sequences used in this study are available upon request. The siRNA sequence of ATR was described previously (24). To establish stable knockdown cells, the retroviral vector pCL-puro-mU6 (a gift from Zhou Songyang, Baylor College of Medicine) was used. The RFWD3 shRNA was based on siRNA no. 1.

In Vivo Ubiquitination Assay. H1299 cells were transfected with HA-ubiquitin, pCMV-p53/pCIN4-Flag-p53, and the E3 ligases. Cells pellets were lysed in SDS buffer (50 mM Tris-Cl, pH 7.5, 1% SDS, 0.5 mM EDTA) and boiled for 10 min. After mild sonication and centrifugation, supernatant was diluted 10 times with NETN buffer (50 mM Tris-Cl, pH 8.0, 150 mM NaCl, 1% NP-40), plus freshly prepared 10 mM iodoacetamide, 1 mM DTT, 10 mM NaF, and protease inhibitors before immunoprecipitation.

G_1 Checkpoint Assay. The G_1 checkpoint assay was performed as described previously (14). The relative S-phase entry was calculated as the ratio of S-phase entry after and before IR.

In Vitro Ubiquitination Assay. The ubiquitination reaction was carried out as described (21). Twenty nanograms of Flag-p53 and 100 ng of E3 (recombinant GST-RFWD3 and/or GST-Mdm2, as indicated) were used in 20 μL of reaction.

ACKNOWLEDGMENTS. We thank Drs. Benjamin Chen (University of Texas Southwestern, Dallas) and Yosef Shiloh (Tel Aviv University) for providing reagents and cell lines and Anna Malovannaya for critical reading of the manuscript. This work was supported in part by grants from National Institutes of Health (GM080703) and Department of Defense (DAMD-W81XWH 04-1-0437) (to Y.W.), CA98500, and Welch Foundation (to J.Q.).

1. Vogelstein B, Lane D, Levine AJ (2000) Surfing the p53 network. *Nature* 408:307–310.
2. Prives C, Hall PA (1999) The P53 pathway. *J Pathol* 187:112–126.
3. Vousden KH, Lane DP (2007) p53 in health and disease. *Nat Rev Mol Cell Biol* 8:275–283.
4. Elledge SJ (1996) Cell cycle checkpoints: Preventing an identity crisis. *Science* 274:1664–1672.
5. Bartek J, Lukas J (2001) Mammalian G1- and S-phase checkpoints in response to DNA damage. *Curr Opin Cell Biol* 13:738–747.
6. Toledo F, Wahl GM (2006) Regulating the p53 pathway: In vitro hypotheses, in vivo veritas. *Nat Rev Cancer* 6:909–923.
7. Brooks CL, Gu W (2006) p53 ubiquitination: Mdm2 and beyond. *Mol Cell* 21:307–315.
8. De Oca Luna RM, Wagner DS, Lozano G (1995) Rescue of early embryonic lethality in mdm2-deficient mice by deletion of p53. *Nature* 378:203–206.
9. Jones SN, et al. (1995) Rescue of embryonic lethality in Mdm2-deficient mice by absence of p53. *Nature* 378:206–208.
10. Barak Y, et al. (1993) mdm2 expression is induced by wild type p53 activity. *EMBO J* 12:461–468.
11. Stommel JM, Wahl GM (2004) Accelerated MDM2 auto-degradation induced by DNA-damage kinases is required for p53 activation. *EMBO J* 23:1547–1556.
12. Kruse JP, Gu W (2008) SnapShot: p53 posttranslational modifications. *Cell* 133:930.
13. Matsuoka S, et al. (2007) ATM and ATR substrate analysis reveals extensive protein networks responsive to DNA damage. *Science* 316:1160–1166.
14. Mu JJ, et al. (2007) A proteomic analysis of ataxia telangiectasia-mutated (ATM)/ATM-Rad3-related (ATR) substrates identifies the ubiquitin-proteasome system as a regulator for DNA damage checkpoints. *J Biol Chem* 282:17330–17334.
15. Chehab NH, et al. (1999) Phosphorylation of Ser-20 mediates stabilization of human p53 in response to DNA damage. *Proc Natl Acad Sci USA* 96:13777–13782.
16. Shimizu H, et al. (2002) The conformationally flexible S9-S10 linker region in the core domain of p53 contains a novel MDM2 binding site whose mutation increases ubiquitination of p53 in vivo. *J Biol Chem* 277:28446–28458.
17. Wallace M, et al. (2006) Dual-site regulation of MDM2 E3-ubiquitin ligase activity. *Mol Cell* 23:251–263.
18. Yu GW, et al. (2006) The central region of HDM2 provides a second binding site for p53. *Proc Natl Acad Sci USA* 103:1227–1232.
19. Canman CE, et al. (1998) Activation of the ATM kinase by ionizing radiation and phosphorylation of p53. *Science* 281:1677–1679.
20. Maya R, et al. (2001) ATM-dependent phosphorylation of Mdm2 on serine 395: Role in p53 activation by DNA damage. *Gene Dev* 15:1067–1077.
21. Li M, et al. (2003) Mono- versus polyubiquitination: Differential control of p53 fate by Mdm2. *Science* 302:1972–1975.
22. Wang Y, et al. (2000) BASC, a super complex of BRCA1-associated proteins involved in the recognition and repair of aberrant DNA structures. *Gene Dev* 14:927–939.
23. Jung SY, et al. (2005) Proteomic analysis of steady-state nuclear hormone receptor coactivator complexes. *Mol Endocrinol* 19:2451–2465.
24. Wang Y, Qin J (2003) MSH2 and ATR form a signaling module and regulate two branches of the damage response to DNA methylation. *Proc Natl Acad Sci USA* 100:15387–15392.